J. Fluid Mech. (1970), *vol.* 45, *part* 1, *pp.* 13–31
Printed in Great Britain

Unsteady viscous flow in a curved pipe

By W. H. LYNE
Department of Mathematics, Imperial College, London S.W. 7†

(Received 25 January 1970 and in revised form 20 July 1970)

The flow in a pipe of circular cross-section which is coiled in a circle is studied, the pressure gradient along the pipe varying sinusoidally in time with frequency ω. The radius of the pipe a is assumed small in relation to the radius of curvature of its axis R. Of special interest is the secondary flow generated by centrifugal effects in the plane of the cross-section of the pipe, and an asymptotic theory is developed for small values of the parameter $\beta = (2\nu/\omega a^2)^{\frac{1}{2}}$, where ν is the kinematic viscosity of the fluid. The secondary flow is found to be governed by a Reynolds number $R_s = \overline{W}^2 a/R\omega\nu$, where $\overline{W}$ is a typical velocity along the axis of the pipe, and asymptotic theories are developed for both small and large values of this parameter. For sufficiently small values of β it is found that the secondary flow in the interior of the pipe is in the opposite sense to that predicted for a steady pressure gradient, and this is verified qualitatively by an experiment described at the end of the paper.

1. Introduction

In this paper we study the flow of an incompressible viscous fluid through a pipe of circular cross-section, which is coiled in a circle. Of special interest is the secondary flow, induced in the plane of the cross-section of the pipe by centrifugal effects.

The steady problem of this kind was first analyzed by Dean (1927, 1928), who found that the motion depended on a parameter K, equal to $2Re^2a/R$, Re being a Reynolds number for flow along the pipe, a the radius of the pipe and R the radius of curvature of its axis. The analysis employed by Dean was restricted to small values of K, but recently this has been extended numerically to moderately large values of K by McConalogue & Srivastava (1968); earlier Barua (1963) had developed an asymptotic boundary-layer theory for very large values of this parameter.

The knowledge of steady flow through a curved pipe is thus quite extensive. On the other hand, time-dependent viscous flows in a curved pipe have not been studied, at least to the author's knowledge. Thus, in this paper, an attempt is made to study the effects of unsteadiness of the motion.

In order to simplify the problem, the radius of curvature of the pipe is assumed large in relation to its own radius, and the pressure gradient applied along the pipe is assumed to be sinusoidal in time with zero mean. This may be realized by the insertion of a pump into the circle in which the pipe is bent, or, alternatively,

† Present address: E.C.L.P. and Co. Ltd., St Austell, Cornwall.

the problem may be reformulated so that the pipe itself performs torsional oscillations; for practical purposes, however, the pipe may be regarded as being bent into a spiral of small pitch, with a pump placed at one of its ends. In §2 the equations of motion are derived and the flow, being unsteady, is seen to depend on two parameters, which are conveniently taken as

$$\epsilon^2 = \frac{\overline{W}^2}{Ra\omega^2}, \quad R_s = \frac{\overline{W}^2}{R\omega}\frac{a}{\nu}; \tag{1.1}$$

here $\overline{W}$ is a typical velocity along the pipe, ω is the frequency and ν the kinematic viscosity of the fluid. The parameter ϵ^2 may be recognized as the ratio of the square of the particle displacement amplitude of the motion along the pipe, to the product of the radius of the pipe and its radius of curvature. The parameter ϵ^2 is taken to be small throughout this paper and this allows the equations to be simplified, thus making the problem more amenable to analysis. It will be seen later that R_s plays the role of a conventional Reynolds number for the secondary flow. This choice of parameters was made to allow direct comparison with the analogous two-dimensional problem of flow induced by a body oscillating in an unbounded viscous fluid, as described by Riley (1967) in a review article. Another parameter of importance in the analysis is

$$\beta^2 = 2\nu/\omega a^2 = 2\epsilon^2/R_s \tag{1.2}$$

and this also is assumed small. Clearly β represents the ratio of the Stokes layer thickness, say $(2\nu/\omega)^{\frac{1}{2}}$, to the radius of the pipe. The smallness of β implies that, for the flow down the pipe, viscous effects are confined to a thin layer on the wall, while the main part of the flow is inviscid.

In §3 a solution is developed by the use of two matched asymptotic expansions, one expansion being valid near to the wall of the pipe where a Stokes shear-wave layer exists and the other expansion being valid in the region away from the wall, in the interior of the pipe. The expansion parameter in each case is β, and a common region of validity is assumed in which the matching takes place. In §4 these expansions have been taken to $O(\beta)$ in both regions where $R_s \ll O(1)$, but when $R_s \gg O(1)$ a solution to only $O(\beta^0)$ has been attempted for the interior, and is described in §5.

In the latter case it is found that a secondary boundary layer of thickness $O(aR_s^{-\frac{1}{2}})$ is formed at the edge of the Stokes layer, in which the velocity of the secondary motion is adjusted to the value dictated by the flow in the core of the pipe. This core is inviscid, and differs from the interior in that the latter contains the secondary boundary layer as well as the core.

As the governing equations for the secondary motion in the interior are steady to first order in β, and the streamlines of the motion are closed, the secondary flow in the core of the pipe must, to first order, have uniform vorticity (see Batchelor 1956). Because of symmetry about that diameter lying in the plane in which the pipe is coiled, the vorticity immediately above this diameter must be equal in magnitude, but of opposite sign, to that immediately below it. Harper (1963) has shown that this leads to the formation of a free boundary layer of thickness $O(aR_s^{-\frac{1}{2}})$ along this diameter. The equations of these boundary layers are then linearized by assuming the velocities of the secondary motion in the

layers are small perturbations to the velocities of the motion in the core. These linearized equations are then solved to give an integral equation for the velocity profile at some station, the strength of the vortex in the core appearing as an eigenvalue. This equation is solved numerically, and the eigenvalue found.

In §6 the results are discussed, the most striking feature being that, at least for sufficiently small values of the parameter β, the secondary flow in the interior of the pipe is in the opposite sense to that predicted for steady flow along the pipe. Thus, whereas the intuitive idea of 'outwards centrifuging' is valid for steady flow, it is not valid in the unsteady flow that we discuss; rather the apparent 'centrifuging' is negative and is therefore directed inwards! This has been verified experimentally using the apparatus described in §7 which was kindly made available by the Physiological Flow Studies Unit at Imperial College.

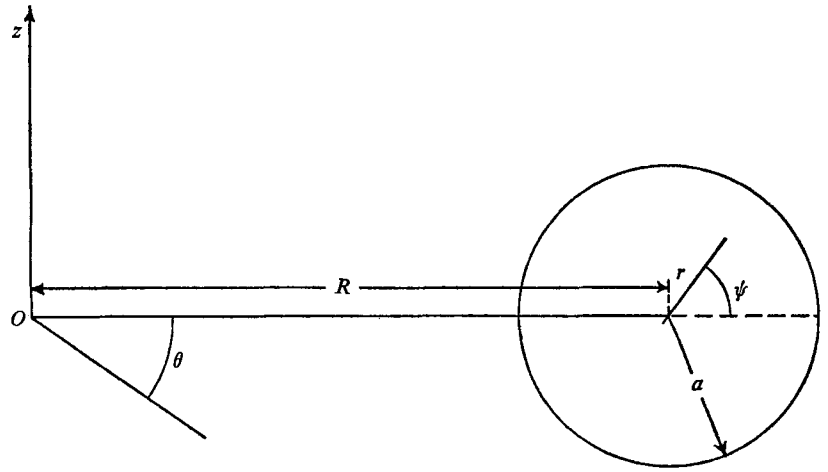

FIGURE 1. The co-ordinate system.

2. The equations of motion

Let us consider incompressible viscous flow in a pipe of circular cross-section and of radius a, the pipe itself being coiled in a circle of radius R about the axis Oz (figure 1). Distance down the pipe is measured by $R\theta$, where θ is the angle which an axial plane (containing Oz) makes with some fixed axial plane. Within the pipe cross-section, polar co-ordinates r, ψ are used. Moreover, the velocity of components corresponding to (r, ψ, θ) are (u, v, w), which are assumed to be independent of θ; in addition p denotes pressure, ρ the density, ν the kinematic viscosity and t the time.

The steady Navier–Stokes equations in these co-ordinates were given by Dean (1927, 1928), the unsteady form following directly as

$$\frac{\partial u}{\partial t}+u\frac{\partial u}{\partial r}+\frac{v}{r}\frac{\partial u}{\partial \psi}-\frac{v^2}{r}-\frac{w^2\cos\psi}{R+r\cos\psi}$$
$$=-\frac{\partial}{\partial r}(p/\rho)-\nu\left(\frac{1}{r}\frac{\partial}{\partial \psi}-\frac{\sin\psi}{R+r\cos\psi}\right)\left(\frac{\partial v}{\partial r}+\frac{v}{r}-\frac{1}{r}\frac{\partial u}{\partial \psi}\right), \quad (2.1)$$

$$\frac{\partial v}{\partial t}+u\frac{\partial v}{\partial r}+\frac{v}{r}\frac{\partial v}{\partial \psi}+\frac{uv}{r}+\frac{w^2\sin\psi}{R+r\cos\psi}$$
$$=-\frac{1}{r}\frac{\partial}{\partial\psi}(p/\rho)+\nu\left(\frac{\partial}{\partial r}+\frac{\cos\psi}{R+r\cos\psi}\right)\left(\frac{\partial v}{\partial r}+\frac{v}{r}-\frac{1}{r}\frac{\partial u}{\partial\psi}\right), \quad (2.2)$$

and
$$\frac{\partial w}{\partial t}+u\frac{\partial w}{\partial r}+\frac{v}{r}\frac{\partial w}{\partial\psi}+\frac{uw\cos\psi}{R+r\cos\psi}-\frac{vw\sin\psi}{R+r\cos\psi}$$
$$=-\frac{1}{R+r\cos\psi}\frac{\partial}{\partial\theta}(p/\rho)+\nu\left[\left(\frac{\partial}{\partial r}+\frac{1}{r}\right)\left(\frac{\partial w}{\partial r}+\frac{w\cos\psi}{R+r\cos\psi}\right)\right.$$
$$\left.+\frac{1}{r}\frac{\partial}{\partial\psi}\left(\frac{1}{r}\frac{\partial w}{\partial\psi}-\frac{w\sin\psi}{R+r\cos\psi}\right)\right]. \quad (2.3)$$

The equation of continuity is

$$\frac{\partial u}{\partial r}+\frac{u}{r}+\frac{u\cos\psi}{R+r\cos\psi}+\frac{1}{r}\frac{\partial v}{\partial\psi}-\frac{v\sin\psi}{R+r\cos\psi}=0. \quad (2.4)$$

We now impose a single sinusoidal pressure gradient along the pipe

$$-\partial(p/\rho)/\partial\theta=R\overline{W}\omega\cos\omega t, \quad (2.5)$$

where $\overline{W}$ has the dimensions of velocity and ω is the angular frequency. We may first note that the exact solution to (2.1), (2.2), (2.3) and (2.4), in the absence of viscosity, is the potential flow solution

$$w=\frac{R\overline{W}\sin\omega t}{R+r\cos\psi}. \quad (2.6)$$

There are no components of secondary flow in the plane of the cross-section, there being a balance between the centrifugal force exerted by the flow along the pipe, and the pressure gradient in that plane. When viscosity is present, however, we may expect a Stokes shear-wave layer of thickness $O(\nu/\omega)^{\frac{1}{2}}$ to be formed at the wall of the pipe, and this is thin when $\omega a^2/\nu$ is large. Within this layer, the value of w will decay to zero as the wall of the pipe is approached, and thus there will no longer be a balance between the centrifugal force and the pressure gradient, because the latter is essentially unchanged. Secondary flow will then be generated within this layer and a consideration of the viscous and centrifugal terms in (2.2) indicate that its magnitude is $O(\overline{W}^2/R\omega)$.

We therefore introduce the following non-dimensional notation:

$$\left.\begin{aligned}\delta=\frac{a}{R},\quad r'=\frac{r}{a},\quad w'=\frac{w}{\overline{W}},\quad u'=\frac{u}{\overline{W}^2/R\omega},\\ v'=\frac{v}{\overline{W}^2/R\omega},\quad \tau=\omega t,\quad p'=\frac{(p+\rho R\theta\overline{W}\cos\omega t)}{\rho\delta\overline{W}^2},\end{aligned}\right\} \quad (2.7)$$

remembering that, in due course, r' and u' will need to be suitably scaled within the Stokes layer.

The momentum equations (2.1), (2.2) and (2.3) now become

$$\frac{\partial u'}{\partial\tau}+\epsilon^2\left(u'\frac{\partial u'}{\partial r'}+\frac{v'}{r'}\frac{\partial u'}{\partial\psi}-\frac{v'^2}{r'}\right)-\frac{w'^2\cos\psi}{1+\delta r'\cos\psi}$$
$$=-\frac{\partial p'}{\partial r'}-\tfrac{1}{2}\beta^2\left(\frac{1}{r'}\frac{\partial}{\partial\psi}-\frac{\delta\sin\psi}{1+\delta r'\cos\psi}\right)\left(\frac{\partial v'}{\partial r'}+\frac{v'}{r'}-\frac{1}{r'}\frac{\partial u'}{\partial\psi}\right), \quad (2.8)$$

$$\frac{\partial v'}{\partial \tau}+\epsilon^2\left(u'\frac{\partial v'}{\partial r'}+\frac{v'}{r'}\frac{\partial v'}{\partial \psi}+\frac{u'v'}{r'}\right)+\frac{w'^2\sin\psi}{1+\delta r'\cos\psi}$$
$$=-\frac{1}{r'}\frac{\partial p'}{\partial \psi}+\tfrac{1}{2}\beta^2\left(\frac{\partial}{\partial r'}+\frac{\delta\cos\psi}{1+\delta r'\cos\psi}\right)\left(\frac{\partial v'}{\partial r'}+\frac{v'}{r'}-\frac{1}{r'}\frac{\partial u'}{\partial \psi}\right), \quad (2.9)$$

and
$$\frac{\partial w'}{\partial \tau}+\epsilon^2\left(u'\frac{\partial w'}{\partial r'}+\frac{v'}{r'}\frac{\partial w'}{\partial \psi}+\frac{u'w'\delta\cos\psi}{1+\delta r'\cos\psi}-\frac{v'w'\delta\sin\psi}{1+\delta r'\cos\psi}\right)$$
$$=\frac{1}{1+\delta r'\cos\psi}\cos\tau+\tfrac{1}{2}\beta^2\left[\left(\frac{\partial}{\partial r'}+\frac{1}{r'}\right)\left(\frac{\partial w'}{\partial r'}+\frac{w'\delta\cos\psi}{1+\delta r'\cos\psi}\right)\right.$$
$$\left.+\frac{1}{r'}\frac{\partial}{\partial \psi}\left(\frac{1}{r'}\frac{\partial w'}{\partial \psi}-\frac{w'\delta\sin\psi}{1+\delta r'\cos\psi}\right)\right]. \quad (2.10)$$

The equation of continuity becomes

$$\frac{\partial u'}{\partial r'}+\frac{u'}{r'}+\frac{u'\delta\cos\psi}{1+\delta r'\cos\psi}+\frac{1}{r'}\frac{\partial v'}{\partial \psi}-\frac{v'\delta\sin\psi}{1+\delta r'\cos\psi}=0. \quad (2.11)$$

In order to simplify the equations and allow some progress to be made, δ is taken to be very small and all terms of $O(\delta)$ are neglected. Equation (2.11) now becomes

$$\frac{\partial u'}{\partial r'}+\frac{u'}{r'}+\frac{1}{r'}\frac{\partial v'}{\partial \psi}=0. \quad (2.12)$$

We satisfy (2.12) by introducing the non-dimensional stream function χ for flow in the cross-section, defined as follows

$$u'=\frac{1}{r'}\frac{\partial \chi}{\partial \psi}, \quad v'=-\frac{\partial \chi}{\partial r'}. \quad (2.13)$$

Eliminating the pressure between (2.8) and (2.9) and neglecting terms of $O(\delta)$, we obtain the vorticity equation for flow in the cross-section:

$$\frac{\partial}{\partial \tau}\nabla^2\chi-\frac{\epsilon^2}{r'}\frac{\partial(\chi,\nabla^2\chi)}{\partial(r',\psi)}-\frac{2}{r'}\left(r'w'\frac{\partial w'}{\partial r'}\sin\psi+w'\frac{\partial w'}{\partial \psi}\cos\psi\right)=\tfrac{1}{2}\beta^2\nabla^4\chi, \quad (2.14)$$

where
$$\nabla^2=\frac{\partial^2}{\partial r'^2}+\frac{1}{r'}\frac{\partial}{\partial r'}+\frac{1}{r'^2}\frac{\partial^2}{\partial \psi^2}; \quad \frac{\partial(a,b)}{\partial(r',\psi)}=\frac{\partial a}{\partial r'}\frac{\partial b}{\partial \psi}-\frac{\partial b}{\partial r'}\frac{\partial a}{\partial \psi}. \quad (2.15)$$

Equation (2.10) becomes, neglecting terms of $O(\delta)$,

$$\frac{\partial w'}{\partial \tau}-\frac{\epsilon^2}{r'}\frac{\partial(\chi,w')}{\partial(r',\psi)}=\cos\tau+\tfrac{1}{2}\beta^2\nabla^2 w'. \quad (2.16)$$

The boundary conditions for (2.14) and (2.16) are

$$\chi=\partial\chi/\partial r'=w'=0 \quad \text{at} \quad r'=1 \quad (2.17)$$

and we shall also require that the solution shall be non-singular within the pipe.

3. The limit $\beta\to 0$

In this section we shall seek solutions to (2.14) and (2.16) which are asymptotic to the exact solutions in the limit $\beta\to 0$, R_s fixed; in later sections we shall study the consequences of taking the further limits $R_s\to 0$ and $R_s\to\infty$. Only periodic dependence on τ will be allowed.

The primes will now be dropped from the dimensionless quantities defined in (2.7) for reasons of simplicity, and all variables are now dimensionless unless stated otherwise.

In the Stokes layer we have seen that the relevant length scale is $(\nu/\omega)^{\frac{1}{2}}$. We therefore introduce the following scaled variables for this region,

$$\eta = \beta^{-1}(1-r), \quad \mathrm{X} = \beta^{-1}\chi, \tag{3.1}$$

and seek solutions to (2.14) and (2.16) for this region of the form

$$w = w_0(\tau, \eta, \psi; R_s) + \beta w_1(\tau, \eta, \psi; R_s) + \beta^2 w_2(\tau, \eta, \psi; R_s) + \ldots, \tag{3.2}$$

$$\mathrm{X} = \mathrm{X}_0(\tau, \eta, \psi; R_s) + \beta \mathrm{X}_1(\tau, \eta, \psi; R_s) + \beta^2 \mathrm{X}_2(\tau, \eta, \psi; R_s) + \ldots, \tag{3.3}$$

subject to the boundary conditions

$$w_i = \mathrm{X}_i = \partial \mathrm{X}_i/\partial\eta = 0, \quad \eta = 0 \quad (i = 0, 1, 2, \ldots). \tag{3.4}$$

In the interior, away from the Stokes layer, we look for solutions of the form

$$w = \sin\tau, \tag{3.5}$$

$$\chi = \chi_0(\tau, r, \psi; R_s) + \beta\chi_1(\tau, r, \psi; R_s) + \beta^2\chi_2(\tau, r, \psi; R_s) + \ldots \tag{3.6}$$

and require that these should match with the solutions in the Stokes layer.

Equation (3.5) is a direct consequence of (2.16) if we note that no steady part of w may exist as there is no preferential direction for the motion; it can be seen to be just the potential flow solution.

Substituting (3.5), and (3.6) into (2.14) and (2.16), and equating like powers of β, we have

$$\frac{\partial}{\partial\tau}\nabla^2\chi_0 = 0, \tag{3.7}$$

$$\frac{\partial}{\partial\tau}\nabla^2\chi_1 = 0, \tag{3.8}$$

$$\frac{\partial}{\partial\tau}\nabla^2\chi_2 - \frac{R_s}{2r}\frac{\partial(\chi_0, \nabla^2\chi_0)}{\partial(r, \psi)} = \tfrac{1}{2}\nabla^4\chi_0. \tag{3.9}$$

Equation (3.7) implies
$$\nabla^2\chi_0 = g_0(r, \psi; R_s) \tag{3.10}$$

and hence
$$\chi_0 = \chi_0^{(u)}(r, \psi, \tau; R_s) + \chi_0^{(s)}(r, \psi; R_s), \tag{3.11}$$

where
$$\nabla^2\chi_0^{(u)} = 0, \tag{3.12}$$

$$\nabla^2\chi_0^{(s)} = g_0(r, \psi; R_s). \tag{3.13}$$

$\chi_0^{(u)}$ contains terms proportional to $e^{in\tau}(n = 1 \text{ to } \infty)$ and has zero time average; $\chi_0^{(s)}$ is independent of τ. Similarly

$$\chi_1 = \chi_1^{(u)}(r, \psi, \tau; R_s) + \chi_1^{(s)}(r, \psi; R_s), \tag{3.14}$$

where
$$\nabla^2\chi_1^{(u)} = 0, \tag{3.15}$$

$$\nabla^2\chi_1^{(s)} = g_1(r, \psi; R_s). \tag{3.16}$$

Substituting (3.1), (3.2) and (3.3) into (2.14) and (2.16) and equating like powers of β, we arrive at the following equations for w_0 and X_0:

$$\frac{\partial w_0}{\partial \tau} = \cos\tau + \frac{1}{2}\frac{\partial^2 w_0}{\partial \eta^2}, \tag{3.17}$$

$$\left(\frac{\partial}{\partial \tau} - \frac{1}{2}\frac{\partial^2}{\partial \eta^2}\right)\frac{\partial^2 \mathrm{X}_0}{\partial \eta^2} = -2w_0\frac{\partial w_0}{\partial \eta}\sin\psi. \tag{3.18}$$

The solution of (3.17) satisfying (3.4) and matching with (3.5) is easily seen to be

$$w_0 = \sin\tau - e^{-\eta}\sin(\tau-\eta). \tag{3.19}$$

Substituting (3.19) into (3.18) and solving, we find that the general solution to (3.18), which has period 2π in τ, may be written as

$$\begin{aligned}\mathrm{X}_0 = \{&-\tfrac{1}{8}e^{-2\eta} - \tfrac{1}{2}\sqrt{2}\,e^{-\eta}\cos(-\eta+\tfrac{1}{4}\pi) - \tfrac{1}{16}\sqrt{2}\,e^{-2\eta}\cos(2\tau-2\eta+\tfrac{1}{4}\pi)\\ &-\tfrac{1}{2}\sqrt{2}\,e^{-\eta}\cos(2\tau-\eta+\tfrac{1}{4}\pi)\}\sin\psi + \mathscr{R}\sum_{n=1}^{\infty} D_n(\psi)\,e^{-\sqrt{n}(1+i)\eta+in\tau}\\ &+B(\psi)\,\eta^3 + C(\psi)\,\eta^2 + F(\tau,\psi)\,\eta + G(\tau,\psi),\end{aligned} \tag{3.20}$$

where terms of exponential growth have been excluded, and $\mathscr{R}$ means 'real part of'. This must match with the solution in the interior, which, written in the variables of the Stokes layer, and using (3.11) and (3.14), becomes

$$\begin{aligned}\mathrm{X} = \beta^{-1}[\chi_0^{(u)}]_{r=1} - \eta[\partial\chi_0^{(u)}/\partial r]_{r=1} + \beta^{-1}[\chi_0^{(s)}]_{r=1}\\ -\eta[\partial\chi_0^{(s)}/\partial r]_{r=1} + [\chi_1^{(u)}]_{r=1} + [\chi_1^{(s)}]_{r=1} + O(\beta).\end{aligned} \tag{3.21}$$

Matching with (3.20) we see that $B(\psi) \equiv C(\psi) \equiv 0$ and this ensures that the tangential velocity of the flow is bounded at the edge of the Stokes layer. This, however, is implicit in our scalings (2.7) which assume that the secondary flow's velocities in the interior of the pipe are of the same order as those in the Stokes layer. If we were to rescale χ we could attempt to match the terms $B\eta^3$ or $C\eta^2$ and this would be equivalent to matching the derivative of the stress or the stress itself. However, detailed arguments demonstrate this would again lead to the conclusion that B and C are identically zero, and hence to the scale of χ used here (see Lyne 1970).

Therefore
$$\chi_0^{(u)}(1,\psi,\tau;R_s) + \chi_0^{(s)}(1,\psi;R_s) = 0 \tag{3.22}$$
and hence
$$\chi_0^{(u)} = 0 \quad \text{on} \quad r = 1. \tag{3.23}$$

The only regular solution to (3.12) with this boundary condition is

$$\chi_0^{(u)} = 0 \tag{3.24}$$

and hence $F(\tau,\psi)$ is a function of ψ only ($F(\psi)$).

From the boundary conditions (3.4) we can deduce

$$\left.\begin{aligned}&D_n(\psi) \equiv 0 \quad (n \neq 2); \quad D_2(\psi) = \tfrac{5}{8}\sin\psi\,e^{\frac{1}{4}i\pi},\\ &F(\psi) = -\tfrac{1}{4}\sin\psi; \quad G(\tau,\psi) = [\tfrac{1}{16}(9\sqrt{2}-10)\cos(2\tau+\tfrac{1}{4}\pi)+\tfrac{5}{8}]\sin\psi.\end{aligned}\right\} \tag{3.25}$$

Hence we have finally

$$\begin{aligned} X_0 = \{ &-\tfrac{1}{4}\eta + \tfrac{5}{8} - \tfrac{1}{8}e^{-2\eta} - \tfrac{1}{2}\sqrt{2}e^{-\eta}\cos(-\eta + \tfrac{1}{4}\pi) + \tfrac{5}{8}e^{-\sqrt{2}\eta}\cos(2\tau - \sqrt{2}\eta + \tfrac{1}{4}\pi) \\ &- \tfrac{1}{16}\sqrt{2}e^{-2\eta}\cos(2\tau - 2\eta + \tfrac{1}{4}\pi) - \tfrac{1}{2}\sqrt{2}e^{-\eta}\cos(2\tau - \eta + \tfrac{1}{4}\pi) \\ &+ \tfrac{1}{16}(9\sqrt{2} - 10)\cos(2\tau + \tfrac{1}{4}\pi)\}\sin\psi. \end{aligned} \tag{3.26}$$

Furthermore, as only periodic dependence on τ is allowed, and (3.24) implies χ_0 is independent of τ, equation (3.9) yields the two equations

$$\frac{\partial}{\partial\tau}\nabla^2\chi_2 = 0, \tag{3.27}$$

$$-\frac{1}{r}\frac{\partial(\chi_0, \nabla^2\chi_0)}{\partial(r, \psi)} = \frac{1}{R_s}\nabla^4\chi_0. \tag{3.28}$$

We see, therefore, that χ_0 satisfies the two-dimensional steady Navier–Stokes equation, with R_s playing the role of a conventional Reynolds number. From the matching condition (3.21), we see that the boundary conditions on χ_0 are

$$\chi_0 = 0, \quad \partial\chi_0/\partial r = \tfrac{1}{4}\sin\psi \quad \text{on} \quad r = 1. \tag{3.29}$$

Having found X_0 and w_0 in the Stokes layer and having derived equations and boundary conditions sufficient to determine χ_0 in the interior, we turn our attention to χ_1 and w_1. As a first step we note that (3.21) implies that the boundary condition on $\chi_1^{(u)}$ is

$$\chi_1^{(u)} = \tfrac{1}{16}(9\sqrt{2} - 10)\cos(2\tau + \tfrac{1}{4}\pi)\sin\psi \quad \text{on} \quad r = 1 \tag{3.30}$$

and the only regular solution of (3.15) which satisfies this boundary condition is

$$\chi_1^{(u)} = \tfrac{1}{16}(9\sqrt{2} - 10)r\cos(2\tau + \tfrac{1}{4}\pi)\sin\psi. \tag{3.31}$$

The equation of $O(\beta^3)$ in the interior yields the two equations

$$\frac{\partial}{\partial\tau}\nabla^2\chi_3 - \frac{R_s}{2r}\frac{\partial(\chi_1^{(u)}, \nabla^2\chi_0)}{\partial(r, \psi)} = 0, \tag{3.32}$$

$$-\frac{1}{r}\frac{\partial(\chi_1^{(s)}, \nabla^2\chi_0)}{\partial(r, \psi)} - \frac{1}{r}\frac{\partial(\chi_0, \nabla^2\chi_1^{(s)})}{\partial(r, \psi)} = \frac{1}{R_s}\nabla^4\chi_1^{(s)}. \tag{3.33}$$

In the Stokes layer the equations for w_1 and X_1 are

$$\frac{\partial w_1}{\partial\tau} - \frac{1}{2}\frac{\partial^2 w_1}{\partial\eta^2} = -\frac{1}{2}\frac{\partial w_0}{\partial\eta}, \tag{3.34}$$

$$\left(\frac{\partial}{\partial\tau} - \frac{1}{2}\frac{\partial^2}{\partial\eta^2}\right)\frac{\partial^2 X_1}{\partial\eta^2} = \frac{\partial^2 X_0}{\partial\tau\,\partial\eta} - \frac{\partial^3 X_0}{\partial\eta^3} - \frac{2\partial(w_0 w_1)}{\partial\eta}\sin\psi, \tag{3.35}$$

and the solution of (3.34) satisfying (3.4) and matching with (3.5) is easily found to be

$$w_1 = -\tfrac{1}{2}\eta e^{-\eta}\sin(\tau - \eta). \tag{3.36}$$

Thus, since X_0 and w_0 are already determined, the inhomogeneous terms in (3.35) are known and we can find the general solution for X_1. However, when we come to determine the unknown constants using the matching equation (3.21) (extended

to include $O(\beta)$ terms) we see that the coefficients of η^2 in the solution X_1 must equal $\frac{1}{2}[\partial^2\chi_0/\partial r^2]_{r=1}$ and this is unknown, since we have not yet tackled the non-linear problem for χ_0 presented by (3.28) and (3.29). X_1 has a form similar to X_0, but is much more lengthy and will not be given here (see Lyne 1970). Its most important feature, however, is its behaviour as $\eta \to \infty$ as this determines matching conditions to be imposed on $\chi_1^{(s)}$:

$$\lim_{\eta\to\infty} X_1 = \{\tfrac{1}{2}\eta - \tfrac{3}{16} - \tfrac{1}{16}(9\sqrt{2}-10)\eta\cos(2\tau+\tfrac{1}{4}\pi) + \tfrac{1}{32}(16\sqrt{2}-21)\cos 2\tau\}\sin\psi + A(\psi)\eta^2. \quad (3.37)$$

We see, from (3.21), that the matching conditions for $\chi_1^{(s)}$, determined from X_0 and X_1, are

$$\chi_1^{(s)} = \tfrac{5}{8}\sin\psi, \quad -\partial\chi_1^{(s)}/\partial r = \tfrac{1}{2}\sin\psi \quad \text{on} \quad r = 1. \quad (3.38)$$

Thus we have again derived equations and boundary conditions sufficient to determine χ_1 in the interior, and we could consider in like fashion the terms of $O(\beta^2)$. This is not pursued here (see Lyne 1970), and instead we proceed with the solution in the interior of the pipe. In order to progress with this it is necessary to consider the limiting forms of the solution when $R_s \to 0$ or $R_s \to \infty$, and this will be our concern in the next two sections.

4. The limit $R_s \to 0$

We now look for a solution that is asymptotic to the exact solution in the further limit $R_s \to 0$.

We therefore try a solution to (3.28) of the form

$$\chi_0 = \chi_{00}(r,\psi) + R_s\chi_{01}(r,\psi) + R_s^2\chi_{02}(r,\psi) + \ldots, \quad (4.1)$$

subject to the matching conditions (3.29), which are now written as

$$\chi_{0i} = 0 \quad (i \geqslant 0); \quad \partial\chi_{00}/\partial r = \tfrac{1}{4}\sin\psi, \quad \partial\chi_{0i}/\partial r = 0 \quad (i \geqslant 1) \quad \text{on} \quad r = 1. \quad (4.2)$$

Substituting (4.1) into (3.28) and equating like powers of R_s, we find as our equation for χ_{00}

$$\nabla^4\chi_{00} = 0. \quad (4.3)$$

The solution of (4.3) which is regular and satisfies (4.2) is found to be

$$\chi_{00} = -\tfrac{1}{8}r(1-r^2)\sin\psi. \quad (4.4)$$

The equation for χ_{01} is

$$\nabla^4\chi_{01} = -\frac{1}{r}\frac{\partial(\chi_{00}, \nabla^2\chi_{00})}{\partial(r,\psi)}, \quad (4.5)$$

whose solution subject to (4.2) is

$$\chi_{01} = -(r^2/3072)(1-r^2)^2\sin 2\psi. \quad (4.6)$$

Similarily χ_{02} is found to be

$$\chi_{02} = -\frac{1}{1,474,560}\{\tfrac{1}{2}r(1-r^2)^2(2-7r^2+4r^4)\sin\psi + r^3(1-r^2)^3\sin 3\psi\} \quad (4.7)$$

and, matching, we can see that $A(\psi)$ in the expression for X_1 (3.37) is

$$A(\psi) = \tfrac{3}{8}\sin\psi - \frac{R_s}{768}\sin 2\psi + \frac{R_s^2}{737,280}\sin\psi + O(R_s^3). \tag{4.8}$$

We solve (3.33) in a similar manner for $\chi_1^{(s)}$, and this is found to be

$$\chi_1^{(s)} = \frac{r}{16}(19-9r^2)\sin\psi + \frac{9}{3072}R_s r^2(1-r^2)^2\sin 2\psi + \frac{R_s^2}{3072}\left\{\frac{1}{1920}(154r-597r^3+840r^5-505r^7+108r^9)\sin\psi + \frac{1}{320}(-r^3-7r^5+17r^7-9r^9)\sin 3\psi\right\} + O(R_s^3). \tag{4.9}$$

5. The limit $R_s \to \infty$

We now seek a solution to (3.28) which is asymptotic to the exact solution for χ_0 in the limit $R_s \to \infty$, and subject to the matching requirements (3.29).

The problem now under consideration is equivalent to that of two-dimensional flow inside a circle whose 'wall' has a tangential velocity $v_w = -0{\cdot}25(\overline{W}^2/R\omega)\sin\psi$. A thin boundary layer of thickness $O(aR_s^{-\frac{1}{2}})$ will be formed at the wall within which, assuming that the layer does not separate, the velocity of the flow is adjusted to that dictated by the flow in the core of the circle. We postulate that in the limit $R_s \to \infty$ no streamlines of the motion in the core enter or leave the boundary layer, thereby causing the flow to have uniform vorticity (see Batchelor 1956). We then solve for the flow in the boundary layer by replacing the non-linear equation by a tractable linear equation, and this gives rise to a velocity distribution at the edge of the core flow which is, for the most part, quite close to a sinusoidal distribution (see figure 3). This gives an *a posteriori* justification for the assumption of the boundary layer not separating, and good grounds on which to argue for the picture of the flow given in figure 2.

The shaded regions within the periphery of the circle denote boundary layers of thickness $O(aR_s^{-\frac{1}{2}})$. A boundary layer is also formed along the line of symmetry $\psi = 0, \pi$ because, when the fluid in the boundary layer at the wall, having started at $\psi = \pi$, reaches $\psi = 0$, it meets boundary-layer fluid from the other semicircle. The two boundary layers impact, and must continue along the line of symmetry. They retain their boundary-layer character because, although the velocity is continuous across the line of symmetry, the vorticity is not, and Harper (1963) has shown that this itself leads to the formation of a boundary layer of thickness $O(aR_s^{-\frac{1}{2}})$ in which to smooth out the discontinuity. The two unshaded regions within the circle comprise the core, and in them the flow has uniform vorticity. The vorticity in one core region has the same magnitude as, but the opposite sign to, the vorticity in the other core region.

We first solve for the flow in the core region of the upper semicircle in figure 2. If we refer to flow in the core by an overbar, the governing equation for $\overline{\chi}_0$ in the core is

$$\nabla^2\overline{\chi}_0 = -\zeta, \tag{5.1}$$

where ζ is the non-dimensional vorticity, which we may expect to be negative from the velocity distribution on the wall of the circle. The boundary condition on $\overline{\chi}_0$ is

$$\overline{\chi}_0 = 0 \quad \text{on} \quad r = 1, \quad \text{or} \quad \psi = 0, \pi. \tag{5.2}$$

The solution of (5.1) subject to (5.2) which is regular everywhere within the circle is found to be

$$\bar{\chi}_0 = \frac{\zeta}{2\pi}\left\{\left[1-\frac{1}{2}\left(r^2+\frac{1}{r^2}\right)\cos 2\psi\right]\tan^{-1}\left(\frac{2r\sin\psi}{1-r^2}\right)\right.$$
$$-\frac{1}{4}\left(r^2-\frac{1}{r^2}\right)\sin 2\psi\log\left(\frac{1+2r\cos\psi+r^2}{1-2r\cos\psi+r^2}\right)$$
$$\left.+\left(r-\frac{1}{r}\right)\sin\psi-\tfrac{1}{2}\pi r^2(1-\cos 2\psi)\right\} \tag{5.3}$$

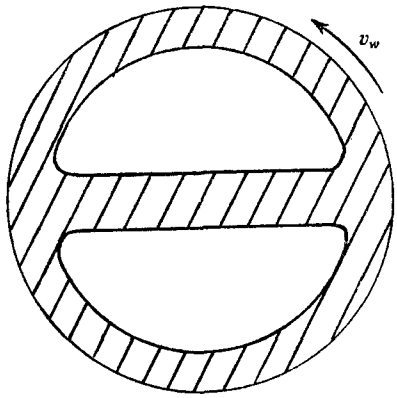

FIGURE 2. Model for flow in the outer regions when R_s is large. Shaded regions denote boundary layers; unshaded regions have uniform vorticity. $v_w = -0{\cdot}25(\overline{W}^2/R\omega)\sin\psi$.

and this gives as our flow velocity at the edge of the core

$$[\bar{v}]_{r=1} = \bar{v}_1 = (\zeta/\pi)(\pi\sin^2\psi - 2\sin\psi - \sin 2\psi\log\tan\tfrac{1}{2}\psi). \tag{5.4}$$

The boundary-layer equation for the layer adjacent to the pipe wall is

$$v\frac{\partial v}{\partial\psi}+u\frac{\partial v}{\partial r} = \bar{v}_1\frac{d\bar{v}_1}{d\psi}+R_s^{-1}\frac{\partial^2 v}{\partial r^2}. \tag{5.5}$$

We now linearize (5.5) in a manner analogous to that employed by Moore (1963) in his study of the stress-induced boundary layer at the surface of a spherical bubble; the subsequent analysis follows closely that of Harper & Moore (1968), who studied the flow field associated with a spherical drop. Moore's linearization is, however, formally justified in the limit $R_s\to\infty$, whereas that employed here is not. For reasons to be discussed later we assume that the velocity in the boundary layer is a small perturbation of the velocity in the core and write

$$v = \bar{v}+v_p, \quad u = \bar{u}+u_p, \tag{5.6}$$

where a suffix p denotes a perturbation quantity. Substituting (5.6) into (5.5) and neglecting quadratic terms in the perturbation quantities, we have, as our boundary-layer equation,

$$\bar{v}_1\frac{\partial v_p}{\partial\psi}+v_p\frac{d\bar{v}_1}{d\psi}+(1-r)\frac{d\bar{v}_1}{d\psi}\frac{\partial v_p}{\partial r} = R_s^{-1}\frac{\partial^2 v_p}{\partial r^2}, \tag{5.7}$$

noting that $\bar{v} = \bar{v}_1$ and $\bar{u} = (1-r)dv_1/d\psi$ to a boundary-layer approximation.

We now transform (5.7) into the diffusion equation by the use of the following transformations:

$$\left.\begin{aligned} y &= (-\zeta R_s)^{\frac{1}{2}}\zeta^{-1}\bar{v}_1(1-r), \\ x &= -\zeta^{-1}\int_{\pi}^{\psi}\bar{v}_1 d\psi, \\ \gamma &= \zeta^{-2}\bar{v}_1 v_p. \end{aligned}\right\} \tag{5.8}$$

Equation (5.7) becomes $$\partial\gamma/\partial x = \partial^2\gamma/\partial y^2, \tag{5.9}$$

with the conditions $$\left.\begin{aligned} &\gamma \to 0 \quad (y\to\infty), \\ &\gamma(x,0) = \zeta^{-2}(v'_w - \bar{v}_1)\bar{v}_1, \end{aligned}\right\} \tag{5.10}$$

and some initial condition $\gamma(0,y)$, which will be discussed later. v'_w is the non-dimensional velocity of the wall of the circle and is equal to $-0{\cdot}25\sin\psi$. The solution of (5.9) subject to the above conditions is given in Carslaw & Jaeger (1959):

$$\gamma(x,y) = \frac{1}{2(\pi x)^{\frac{1}{2}}}\int_0^{\infty}\gamma(0,y')\{e^{-(y-y')^2/4x} - e^{-(y+y')^2/4x}\}dy' + \frac{2}{\sqrt{\pi}}\int_{y/2\sqrt{x}}^{\infty}(x - y^2/4\mu^2, 0)e^{-\mu^2}d\mu. \tag{5.11}$$

The boundary-layer equation for the layer along the line of symmetry $\psi = 0, \pi$ can be written as

$$u\frac{\partial u}{\partial s} + v\frac{\partial u}{\partial n} = \bar{u}_1\frac{d\bar{u}_1}{ds} + R_s^{-1}\frac{\partial^2 u}{\partial n^2}, \tag{5.12}$$

where s is the non-dimensional co-ordinate along the line $\psi = 0$ and π, and $s = 0$ is $\psi = 0$, and n is the non-dimensional co-ordinate normal to it. u and v are the non-dimensional velocities associated with the new co-ordinates. Thus u is in the direction of s increasing and v is in the direction of n increasing. $\bar{u}_1$ is the velocity of the flow in the core at $n = 0$ and is equal to $(1/r)|\partial\bar{\chi}_0/\partial\psi|$ evaluated at $\psi = 0$ or π.

Using (5.6) and linearizing as before, we have as our linearized boundary-layer equation

$$\bar{u}_1\frac{\partial u_p}{\partial s} + u_p\frac{d\bar{u}_1}{ds} - n\frac{d\bar{u}_1}{ds}\frac{\partial u_p}{\partial n} = R_s^{-1}\frac{\partial^2 u}{\partial n^2}. \tag{5.13}$$

Employing the following transformations:

$$\left.\begin{aligned} Y &= -(-\zeta R_s)^{\frac{1}{2}}\zeta^{-1}\bar{u}_1 n, \\ X &= -\zeta^{-1}\int_0^{s}\bar{u}_1 ds, \\ \Gamma &= \zeta^{-2}\bar{u}_1 u_p, \end{aligned}\right\} \tag{5.14}$$

we again arrive at the diffusion equation

$$\partial\Gamma/\partial X = \partial^2\Gamma/\partial Y^2. \tag{5.15}$$

The perturbation vorticity to a boundary-layer approximation is

$$(-\zeta R_s)^{\frac{1}{2}}\zeta\Theta = (-\zeta R_s)^{\frac{1}{2}}\zeta\,\partial\Gamma/\partial Y \tag{5.16}$$

and this also satisfies the diffusion equation

$$\partial\Theta/\partial X = \partial^2\Theta/\partial Y^2. \tag{5.17}$$

To ensure zero vorticity along $\psi = 0, \pi$ we therefore solve (5.17) subject to the boundary conditions

$$\left.\begin{aligned} &\Theta \to 0 \quad \text{as} \quad Y \to \infty, \\ &\Theta = (-\zeta R_s)^{-\frac{1}{2}} \quad \text{on} \quad Y = 0, \end{aligned}\right\} \tag{5.18}$$

and some initial condition $\Theta\,(0, Y)$.

As before we find

$$\Theta(X, Y) = \frac{1}{2(\pi X)^{\frac{1}{2}}}\int_0^\infty \Theta(0, Y')\{e^{-(Y-Y')^2/4X} - e^{-(Y+Y')^2/4X}\}\,dY' + (-\zeta R_s)^{-\frac{1}{2}}\operatorname{erfc}\left(\frac{Y}{2\sqrt{X}}\right). \tag{5.19}$$

Neglecting the term of $O(R_s^{-\frac{1}{2}})$ and integrating once, we have

$$\Gamma(X, Y) = \frac{1}{2(\pi X)^{\frac{1}{2}}}\int_0^\infty \Gamma(0, Y')\{e^{-(Y-Y')^2/4X} + e^{-(Y+Y')^2/4X}\}\,dY'. \tag{5.20}$$

Let a suffix e denote the end of each boundary layer. Thus x_e is equivalent to $\psi = 0$ for the layer along the circle wall, and X_e is equivalent to $\psi = \pi, r = 1$ for the layer along the line of symmetry. We now assume that the velocity profiles at the end of each layer are convected around the corners without change, an assumption which will be discussed later. Therefore, noting that $y \equiv Y$ at the corners, we find that

$$\left.\begin{aligned} \gamma(x_e, y) &\equiv \Gamma(0, Y), \\ \Gamma(X_e, Y) &\equiv \gamma(0, y). \end{aligned}\right\} \tag{5.21}$$

Because of (5.21), (5.11) and (5.20) are a pair of linked integral equations for the velocity perturbation in the boundary layer. Looking at the point x_e, and substituting (5.20) into (5.11), using (5.21), and performing one integration, we arrive at the following integral equation for the profile of γ at x_e:

$$\gamma(x_e, y) = \frac{1}{2[\pi(x_e + X_e)]^{\frac{1}{2}}}\int_0^\infty (x_e, y')\,e^{-y'^2/4X_e - y^2/4x_e}\{e^{\alpha^2}\operatorname{erf}(\alpha) - e^{\beta^2}\operatorname{erf}(\beta)\}\,dy' + \frac{2}{\sqrt{\pi}}\int_{y/2\sqrt{x_e}}^\infty \gamma(x_e - y^2/4\mu^2, 0)\,e^{-\mu^2}\,d\mu, \tag{5.22}$$

where

$$\alpha = \left(\frac{y'}{4X_e} + \frac{y}{4x_e}\right)\left(\frac{4x_eX_e}{x_e + X_e}\right)^{\frac{1}{2}}, \quad \beta = \left(\frac{y'}{4X_e} - \frac{y}{4x_e}\right)\left(\frac{4x_eX_e}{x_e + X_e}\right)^{\frac{1}{2}}. \tag{5.23}$$

The unknown constant ζ appears in the known second integral on the right-hand side of (5.22), and is found when we apply the condition $\gamma \to 0$ as $y \to \infty$.

The equation (5.22) was solved numerically for $\gamma(x_e, y)$ by iteration. A more convenient form for the numerical evaluation of the second integral on the right-hand side of (5.22) was found to be

$$\frac{y}{2\sqrt{\pi}}\int_0^{x_e} \frac{\gamma(x, 0)}{(x_e - x)^{\frac{3}{2}}}\,e^{-y^2/4(x_e - x)}\,dx = \frac{y}{2\sqrt{\pi}}\int_\pi^0 \frac{(-\zeta^{-1})\bar{v}_1\gamma(x(\psi), 0)}{(x_e - x(\psi))^{\frac{3}{2}}}\,e^{-y^2/4(x_e - x(\psi))}\,d\psi, \tag{5.24}$$

and when this was evaluated by Simpson's rule using a step length of $\pi/200$, and the other integral evaluated by Simpson's rule using a step length of 0·1, the profile was given correct to three significant figures after convergence of the iterations. Infinity was taken to be 10 and this was found more than adequate.

Applying the condition that $\gamma \to 0$ when $y \to \infty$, ζ was found to be $-0{\cdot}56$.

We may now attempt to justify the linearization. If we plot $-v'_w$ and $-\bar{v}_1$ against ψ as in figure 3, we see that their difference, which is a measure of the perturbation velocity, is quite small compared with $-\bar{v}_1$ for a significant part of the boundary layer. Of course, the perturbation cannot be small near $\psi = 0$ (or π) as $\bar{v}_1 \sim \psi \log \frac{1}{2}\psi$ when ψ is small, but we hope this will not alter the result significantly.

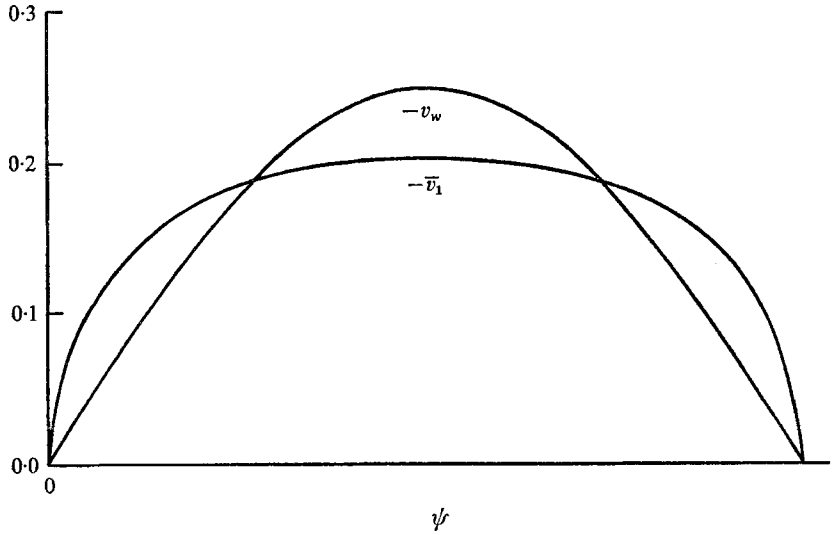

FIGURE 3. Comparison of the velocity distribution at the edge of the core flows v_1, with the distribution on the wall of the circle v'_w.

To return to the assumption contained in (5.21), we find, on closer analysis, that $\bar{\chi}_0$ is, for the most part, dominated by an irrotational term in each corner. Further, we find that, if the linearization is still valid, then the perturbation vorticity is convected around each corner on the streamlines of this motion, and this leads directly to the conclusion (5.21). This analysis is given in detail in Lyne (1970), and we may remark that it follows closely that of Harper (1963) and Moore (1963). In addition Stewartson (1957) described the same type of phenomenon in connexion with the boundary layer on a rotating sphere.

6. Results

As can be seen from the solutions to χ_0, both for small and large values of R_s, the flow in the interior is steady in the limit $\beta \to 0$, and in the opposite sense to that predicted for a steady pressure gradient along the pipe. (See Dean 1927, 1928; Barua 1963; and McConalogue & Srivastava 1968.) That is the motion along the line of symmetry $\psi = 0$, π is from the outer side of the pipe to the

inner. The reason seems to be that 'centrifuging' generates motion which is entirely confined to the Stokes layer. The fluid is driven along the wall from the outer side of the bend to the inner, under the action of the pressure gradient which, in the Stokes layer, is no longer balanced by the centrifugal force associated with flow along the pipe; it returns centrifugally within, and at the edge of, the Stokes layer only, and in so doing 'drags' the fluid in the interior around in the manner found. A sketch of the mean first-order streamlines in figure 4 makes this clear. It is interesting to see to what extent the picture, given by the theory developed above, is complete.

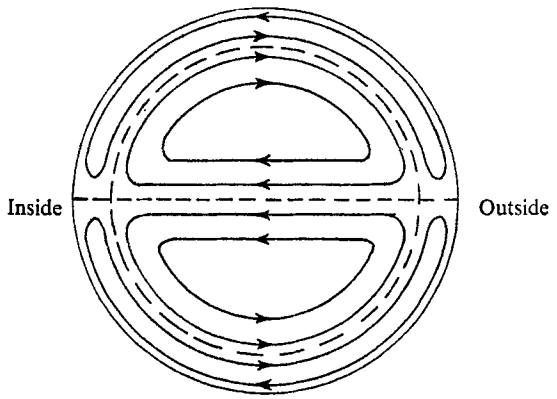

FIGURE 4. Sketch of the streamlines in the plane of the cross-section for small β.

Taking the first-order solution for flow in the interior χ_0, and plotting its vorticity at $\psi = \frac{1}{2}\pi$ for different values of R_s, we arrive at the situation in figure 5. The expression used for the non-dimensional vorticity ζ at $\psi = \frac{1}{2}\pi$ with R_s small is

$$\zeta = -\nabla^2\chi_{00} - R_s^2\nabla^2\chi_{02}. \tag{6.1}$$

The error involved is $O(R_s^4)$, because $\nabla^2\chi_{03}$ (like $\nabla^2\chi_{01}$) is identically zero on $\psi = \frac{1}{2}\pi$. As can be seen from both figure 5 and §4, the $O(R_s^2)$ term in (6.1) is considerably smaller than the $O(1)$ term for values of R_s up to 100. Therefore this expression should be a good asymptotic representation of ζ for these values of R_s, and, if we bear in mind that the error is $O(R_s^4)$, the vorticity profile for $R_s = 200$ is perhaps not without significance. It shows clearly the development of a core of uniform vorticity as R_s increases, but perhaps indicates that the magnitude of the vorticity when $R_s \to \infty$ has been over-estimated because of our crude linearization.

However, it is worth observing that if the wall of the circle in §5 moves with a speed $\bar{v}_1$, this being the velocity at the semicircular edge of the core flow, then no boundary layer is formed at the wall of the circle, and any effect due to the vorticity discontinuity along the line of symmetry is $O(R_s^{-\frac{1}{2}})$ which is neglected. If ζ is now chosen so that the average velocity at the circle wall is the same as for the problem under consideration, i.e.

$$\begin{aligned} -\frac{1}{4}\int_0^\pi \sin\psi\, d\psi &= \int_0^\pi \bar{v}_1 d\psi \\ &= \frac{\zeta}{\pi}\int_0^\pi (\pi\sin^2\psi - 2\sin\psi - \sin 2\psi \log\tan\tfrac{1}{2}\psi)\, d\psi, \end{aligned} \tag{6.2}$$

then we find $\zeta = -0{\cdot}535$. This figure is reassuringly close to that predicted both by the linearized boundary-layer theory developed in §5 for large R_s and by the shape of the low R_s vorticity curve for $R_s = 200$.

In addition Kuwahara & Imai (1969) have recently computed the solution to the full equations for χ_0 using values of R_s up to 2048. They find that at the latter value the vorticity is $\zeta = -0{\cdot}54$, and this gives considerable support both to our value of $-0{\cdot}56$ as $R_s \to \infty$ and to our confidence in the linearization of §5.

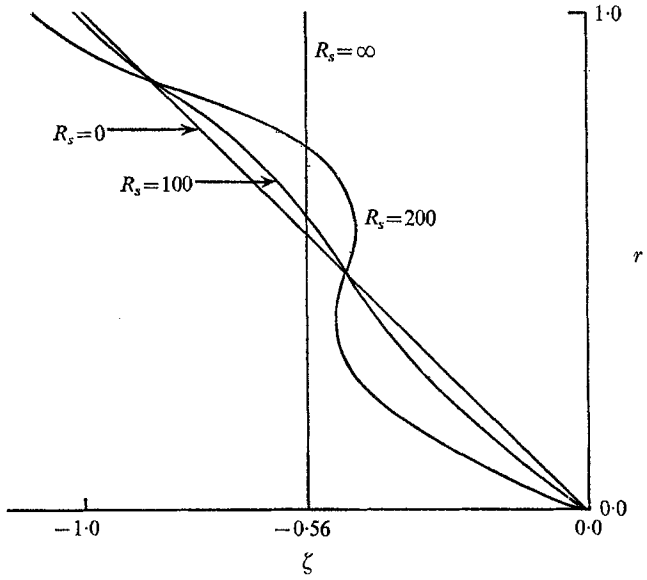

FIGURE 5. Vorticity profiles when $\psi = \frac{1}{2}\pi$ for different values of R_s.

It is of interest to locate the precise position of that stagnation point which represents the vortex centre (r_c, ψ_c) of the flow in the interior. Solving for small R_s and neglecting terms of $O(\beta)$ we find

$$\left.\begin{aligned} r_c &= \tfrac{1}{3}\sqrt{3} - \sqrt{3}\, R_s^2/1{,}658{,}880 + O(R_s^4), \\ \psi_c &= \tfrac{1}{2}\pi - \sqrt{3}\, R_s/864 + O(R_s^3). \end{aligned}\right\} \tag{6.3}$$

On the other hand, as $R_s \to \infty$ the centre tends to $(0{\cdot}48, \frac{1}{2}\pi)$. Thus the vortex centre moves in the direction of the fluid motion at the semicircular edge of the vortex, before inertial effects become dominant and return the centre to the line $\psi = \frac{1}{2}\pi$. Similar results have been obtained by Burggraf (1966) and Kuwahara & Imai (1969).

If we had allowed β in this theory to take any value, then $\beta \to \infty$ would correspond to the steady state with concomitant positive centrifuging, i.e. the flow along the line $\psi = 0$, π would be from the inside of the bend to the outside. However, for $\beta > 0{\cdot}11$ but small enough to be within the range of this theory, the mean flow within the outer region given by the first three terms of the expansion (3.6) to $O(\beta^2)$ and R_s equal to zero, is wholly from the inside to the outside on the line $\psi = \frac{1}{2}\pi$. This shows a tendency towards the solution for the steady problem.

7. Experimental observations

The apparatus consisted of a length of clear plastic tubing bent into one loop of a circular spiral of small pitch and filled with water. A pump, which consisted of a large glass syringe, was attached to one end, and this was driven approximately in simple harmonic motion by an eccentric mounted on the shaft of an electric motor; at the other end of the pipe there was a reservoir. The apparatus is shown by figure 6 in plan view.

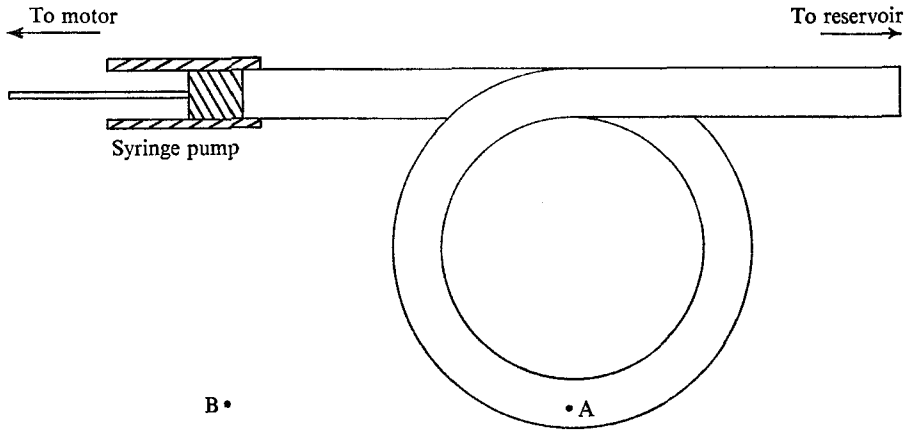

FIGURE 6. The experimental apparatus.

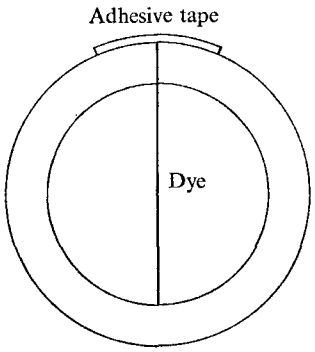

FIGURE 7. Cross-section of pipe after injection of dye.

For an indicator dye a 5 % aqueous solution of amaranth was used, its density being adjusted to that of water by adding a sufficient quantity of alcohol. A streak of dye was injected at A with the apparatus at rest, the streak of dye running from the bottom of the pipe to the top. This was achieved by puncture of the wall of the pipe with the needle of a syringe, which was filled with dye, followed by the drawing out of a streak; after the needle was removed the hole was patched with adhesive tape. A section at A is shown in figure 7 after the injection of dye.

The apparatus was then set in motion, and the movement of the streak observed. The results are discussed later.

The dimensions of the apparatus were as follows: radius of the pipe $a = 0{\cdot}75\,\text{cm}$; radius of the spiral $R = 10{\cdot}0\,\text{cm}$; angular frequency of pump $\omega \simeq 4\pi$ rad s^{-1}; amplitude of pump $= 0{\cdot}5\,\text{cm}$; kinematic viscosity of water $= 0{\cdot}01\,\text{cm}^2\,\text{s}^{-1}$. Thus the basic parameters had the following values:

$$\delta = 0{\cdot}075, \quad \epsilon = 0{\cdot}18, \quad R_s \simeq 24, \quad \beta = 0{\cdot}05.$$

From the magnitude of these parameters we should have expected the flow to look like the situation in figure 4. In fact, only the motion in the interior was observed clearly, but this was not surprising as the Stokes layer was very small.

The photographs in figure 8 (plate 1) were taken at intervals of approximately 3 sec, the camera being positioned at B and above the plane in which the pipe was coiled. It viewed the test section at an angle of approximately 45°, and so the streak of dye was inclined at a similar angle in order to obtain a clearer picture.

As can be seen, in the centre of the pipe the streak of dye was observed to move towards the inside of the bend; at the top and bottom, on the other hand, it moved towards the outside, thus agreeing with the predictions for flow in the outer region.

It should be mentioned that what is observed is the path of each particle of fluid, and so we need to consider the mass-transport velocity of particles in an oscillatory flow. In the present case, the mass-transport velocity field is confined to the plane of the secondary flow, and in the interior the particle paths are found to coincide with the streamlines of the flow to first order in β. In the Stokes layer, however, this is no longer the case, and it is found theoretically that, in addition to the first-order secondary flow calculated in this paper, there is a contribution to the particle velocity of the same order which is parallel to the plane in which the pipe is coiled and whose mean is directed from the inside to the outside of the curve in which the pipe is bent. This contribution decays to zero exponentially at the edge of the Stokes layer, and so its effect is not observed.

The author would like to thank Professor J. T. Stuart for his invaluable help and guidance throughout the course of this work. Thanks are also due to Dr C. G. Caro of the Physiological Flow Studies Unit at Imperial College for the provision of the experimental equipment, and also to Mr P. Ford, Mr M. Blackett and Mr J. P. O'Leary for their ready assistance. The author also acknowledges receipt of a maintenance grant from the Science Research Council.

REFERENCES

BARUA, S. N. 1963 *Quart. J. Mech. Appl. Math.* **16**, 61–77.

BATCHELOR, G. K. 1956 *J. Fluid Mech.* **1**, 177–90.

BURGGRAF, O. R. 1966 *J. Fluid Mech.* **24**, 113–51.

CARSLAW, H. S. & JAEGER, J. C. 1959 *Conduction of Heat in Solids* (2nd edn). Macmillan.

DEAN, W. R. 1927 *Phil. Mag.* (7), **4**, 208–23.

DEAN, W. R. 1928 *Phil. Mag.* (7), **5**, 673–95.

HARPER, J. F. 1963 *J. Fluid Mech.* **17**, 141–53.

HARPER, J. F. & MOORE, D. W. 1968 *J. Fluid Mech.* **32**, 367–91.

KUWAHARA, K. & IMAI, I. 1969 *Phys. Fluids Supplement* II, **12**, 94–101.

LYNE, W. H. 1970 Thesis submitted for Ph.D. University of London.

MCCONALOGUE, D. J. & SRIVASTAVA, R. S. 1968 *Proc. Roy. Soc.* A **307**, 37–53.

MOORE, D. W. 1963 *J. Fluid Mech.* **16**, 161–76.

RILEY, N. 1967 *J. Inst. Maths. Applics.* **3**, 419–34.

STEWARTSON, K. 1957 *Proc. Symp. Boundary Layer Res., Int. Union theoret. appl. Mech. Freiburg i. Br.* pp. 59–71. (Springer, 1968).

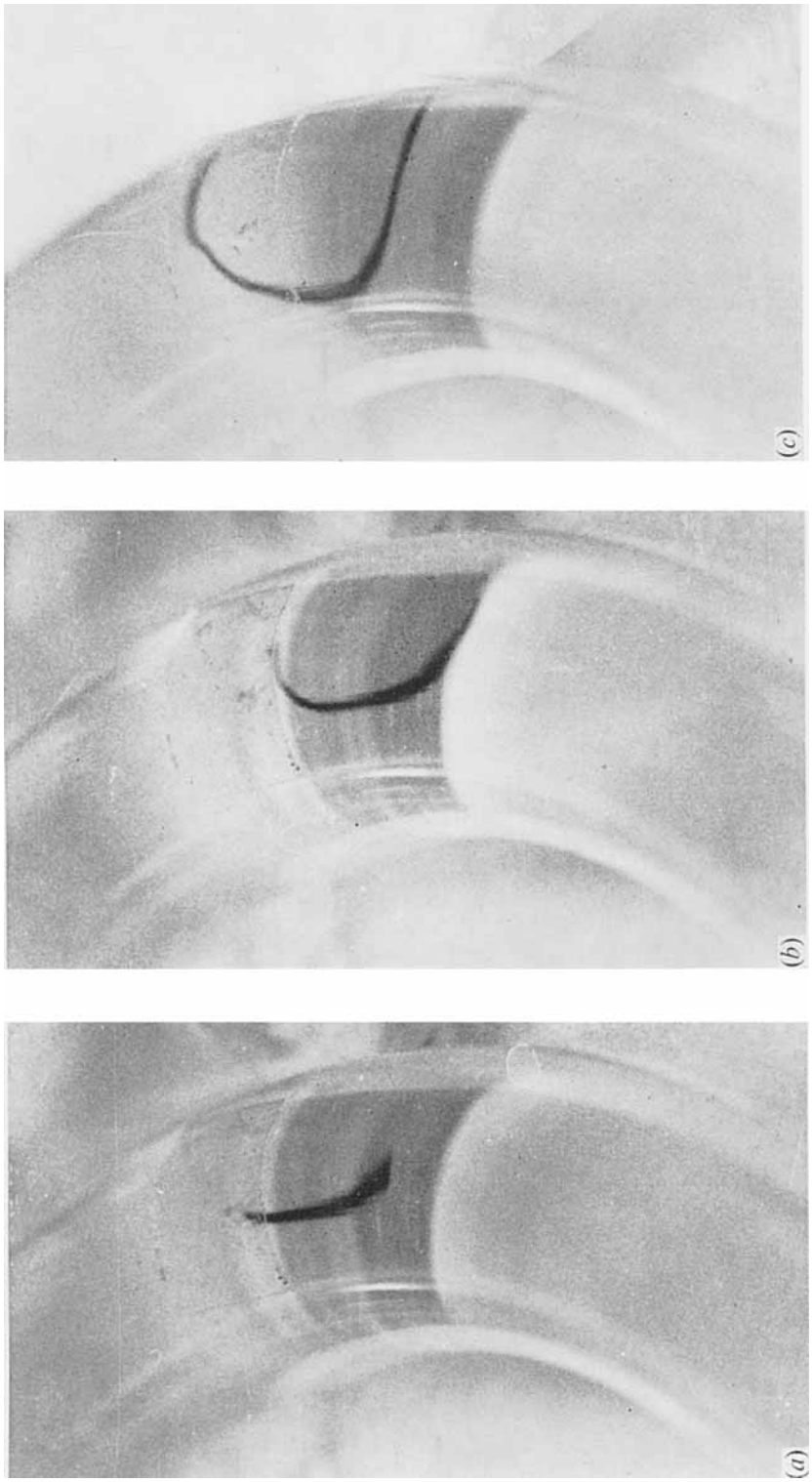

FIGURE 8. Photographs of test section taken at intervals of approximately three seconds.